



AMERICAN METEOROLOGICAL SOCIETY

Journal of Climate

EARLY ONLINE RELEASE

This is a preliminary PDF of the author-produced manuscript that has been peer-reviewed and accepted for publication. Since it is being posted so soon after acceptance, it has not yet been copyedited, formatted, or processed by AMS Publications. This preliminary version of the manuscript may be downloaded, distributed, and cited, but please be aware that there will be visual differences and possibly some content differences between this version and the final published version.

The DOI for this manuscript is doi: 10.1175/JCLI-D-11-00433.1

The final published version of this manuscript will replace the preliminary version at the above DOI once it is available.

If you would like to cite this EOR in a separate work, please use the following full citation:

Li, X., and W. Zhou, 2012: Quasi-four-year Coupling between El Niño-Southern Oscillation and Water Vapor Transport over East Asia-WNP. *J. Climate*. doi:10.1175/JCLI-D-11-00433.1, in press.



1 **Quasi-four-year Coupling between El Niño-Southern Oscillation and**
2 **Water Vapor Transport over East Asia-WNP**

3

4 XIUZHEN LI AND WEN ZHOU

5 Guy Carpenter Asia-Pacific Climate Impact Centre, School of Energy and Environment, City University of Hong

6 Kong, Hong Kong, China

7

8

9

10

11

12

13

Submitted to *Journal of Climate*

14

July 2011

15

16

17

18

19

20

21

22

23

24

25 *Corresponding author address:* Dr. Wen Zhou, School of Energy and Environment, City University

26 of Hong Kong, 2/F, Harbour View 2, 16 Science Park East Avenue, Hong Kong Science Park, Shatin

27 NT.

28 E-mail: wenzhou@cityu.edu.hk

29

ABSTRACT

30 Summer moisture circulation anomaly over East Asia and the western North Pacific (WNP)
31 couples well with the El Niño-Southern Oscillation (ENSO) in a quasi-four-year period. The moisture
32 circulation is dominated by two well-separated modes. The first mode exhibits an anticyclonic
33 (cyclonic) moisture circulation over tropical-subtropical East Asia-WNP, with an easterly (westerly)
34 transport over the tropical WNP-Indian Ocean; the second mode displays an alternating pattern, with an
35 anticyclonic (cyclonic) moisture circulation over the subtropical WNP layered between two cyclonic
36 (anticyclonic) circulations. Both modes couple well with the ENSO signal during its quasi-four-year
37 cycle. Within the cycle, in the summer of a developing warm episode, the positive phase of the second
38 mode plays a key role, while in the transitional summer between a decaying warm episode and a
39 developing cool episode, the positive phase of the first mode tends to take effect. In the summer of a
40 developing cool episode, the negative phase of the second mode plays an important role, while the
41 negative phase of the first mode tends to take effect in the transitional summer between a decaying cool
42 episode and a developing warm episode.

43 The anticyclone (cyclone) over the Philippine Sea region serves as a bridge in the quasi-four-year
44 coupling. Its establishment and eastward extension modify moisture circulation over East Asia-WNP.
45 Conversely, the easterly (westerly) wind to the south of the anticyclone (cyclone) is beneficial for the
46 formation and eastward propagation of the Kelvin wave hence to the development of the quasi-four-
47 year periodic ENSO episode.

48 **1. Introduction**

49 Variability in precipitation has long resulted in either severe floods or droughts,
50 which bring devastating impacts to regional societies and economies (Ding 1992;
51 Kripalani and Kulkarni 2001). The amount of precipitation over a region is
52 determined to some extent by the available moisture; it will not rain at all unless there
53 is a sufficient supply of moisture. Generally, precipitation over any region is derived
54 from two moisture sources: local evaporation and externally advected moisture. It is
55 stated by Benton et al. (1950) and Budyko (1974) that even on the most extensive
56 continents where the relative role of local evaporation is maximized, the majority of
57 precipitation is derived from water vapor of external origin rather than from local
58 evaporation. Hence, the transportation of water vapor by atmospheric circulation
59 plays a vital role in determining rainfall patterns.

60 Water vapor transport over East Asia is extremely complex and energetic. It is
61 dominated jointly by the western Pacific subtropical high (WPSH) and three Asian
62 summer monsoon subsystems: the southwest summer monsoon, the southeast summer
63 monsoon, and the East Asia summer monsoon (EASM), all of which display
64 pronounced year-to-year variation (e.g., Chen et al. 1992; Murakami and Matsumoto
65 1994; Ueda and Yasunari 1996; Wang et al. 2008). Because it is mainly advected by
66 the monsoon flow, water vapor transport over East Asia also exhibits remarkable
67 annual variability (e.g., Simmonds et al. 1999; Zhou and Yu 2005). Though the
68 climatic mean moisture transport over East China is primarily from the Indian Ocean,
69 the water vapor associated with the anomalous precipitation is derived from the
70 western Pacific Ocean instead (Simmonds et al. 1999). Investigation had disclosed
71 that when the Mei-Yu/Baiu rain band was heavier than normal, the anomalous flows
72 originated from the Philippine Sea; when the heavier rain band shifted northward, the

73 anomalous flows came from the East China Sea (Zhou and Yu 2005). Year-to-year
74 variations in westerly moisture transport from the Indian Ocean and southerly
75 moisture transport across the equator had also been investigated, and these variations
76 had been shown to be closely related to different types of precipitation over the
77 western North Pacific (WNP; Hattori et al. 2005, Zhou et al. 2009a). Hence, tying to
78 anomalous precipitation patterns, the moisture circulation over East Asia-WNP
79 experiences remarkable interannual variation.

80 It was pointed out by a number of recent studies that El Niño-Southern
81 Oscillation (ENSO) exhibited a remarkable influence on the interannual variability of
82 the climate over East Asia (e.g., Huang and Wu 1989; Zhang et al. 1996; Feng et al.
83 2010, 2011). During different stages of the ENSO cycle, sea surface temperature
84 (SST) anomalies in the tropical Pacific have different impacts on the summer
85 monsoon and thus the summer rainfall pattern over East Asia-WNP (Yang et al.
86 2004). In the summer of a developing El Niño event, the EASM is weak and above-
87 normal monsoon rainfall is observed in the Yangtze River and Huaihe River valleys,
88 while below-normal rainfall takes place to the south and the north. During the
89 summer of a decaying El Niño event, the EASM tends to be strong and severe
90 flooding may occur to the south of the Yangtze River, while there may be drought in
91 the Yangtze River and Huaihe River valleys. Similarly, La Niña events can also
92 strongly affect the monsoon and rainfall over East Asia, but in the opposite direction
93 (e.g., Huang and Zhou 2002; Huang et al. 2004; Chen 2002). In the study of the
94 mechanisms of ENSO-East Asia climate interaction, an anomalous lower-tropospheric
95 anticyclone was found to develop rapidly over the WNP in the late fall of the year
96 when a strong El Niño event matured (Wang et al. 2000). The anomaly persisted until
97 the ensuing summer, resulting in an enhanced subtropical high, which in turn carried

98 abundant moisture from the WNP to East Asia, causing above-normal rainfall over the
99 middle latitudes extending from the Yangtze River valley to the east of Japan (Zhang
100 2001). Concurrently, warming in the tropical Indian Ocean acted like a capacitor
101 anchoring atmospheric anomalies over the Indo-western Pacific Ocean. It caused a
102 baroclinic Kelvin wave, which induced suppressed convection and the anomalous
103 anticyclone in the subtropical northwest Pacific (Xie et al. 2009). In a La Niña event,
104 the opposite pattern will be found. Hence, significant variation in the atmospheric
105 circulation over East Asia-WNP may occur during different stages of the ENSO cycle,
106 which may significantly affect the transport and divergence of moisture.

107 It is explored that the ENSO's period varies irregularly between 2 and 7 years,
108 with a quite robust average of around 4 years (Macmynowski and Tziperman 2008;
109 Climate Prediction Center 2005). Multichannel singular spectrum analysis (M-SSA)
110 was applied to the equatorial sea surface temperature anomaly (SSTA) and zonal wind
111 (Jiang et al. 1995). It was shown that the quasi-biennial (QB) mode together with the
112 quasi-quadrennial (QQ) mode provided a very good approximation to ENSO events.
113 Although the QQ mode was more fundamental and dominated the variance, more
114 attention had been paid to the QB mode (Rasmusson et al. 1990, Ropelewski et al.
115 1992). Hence, to investigate an area lacking in previous research, this study focuses
116 mainly on the coupling between the interannual variation of summer moisture
117 circulation over East Asia-WNP and ENSO events during a quasi-four-year period.

118 In section 2, the datasets and methodology used in this study are described. The
119 spatial and temporal variations of summer moisture circulation over East Asia-WNP
120 are investigated in section 3. In section 4 the quasi-four-year coupling between ENSO
121 and water vapor transport over East Asia-WNP and the possible mechanisms
122 maintaining this coupling are revealed. Cases studies of this quasi-four-year coupling

123 are examined in section 5. Our discussion and conclusions are presented in section 6.

124

125 **2. Data and methodology**

126 In this study, the 1979–2009 Japanese 25-year Reanalysis Project (JRA-25)
127 dataset¹ is applied. The JRA-25 products have a spectral resolution of T106
128 (equivalent to a horizontal grid size of around 120 km), and 40 vertical layers in a
129 hybrid sigma-pressure coordinate. This dataset provides the foundation for a high-
130 quality analysis of the Asian region. In addition to conventional surface and upper air
131 observations, precipitable water retrieved from orbital satellite microwave radiometer
132 radiance, brightness temperature from the TIROS Operational Vertical Sounder
133 (TOVS), and other satellite data were assimilated using a three-dimensional
134 variational method in the dataset. A detailed description can be found in Onogi et al.
135 (2007). The variables employed are monthly specific humidity, wind fields, and
136 vertically integrated water vapor flux.

137 To determine the relationship between the sea surface temperature and moisture
138 transport, the monthly extended reconstructed sea surface temperature version 3b
139 (ERSST V3b; Smith et al. 2008), with a resolution of 2° latitude × 2° longitude, was
140 employed. The Oceanic Niño Index (ONI; 3 months running mean of SSTA in the
141 Niño 3 region [5°S–5°N, 120–170°W])² was also employed in this study. The time
142 range of these two datasets is from the winter of 1978 to the spring of 2010.

143 To determine the spatial and temporal patterns of summer moisture circulation
144 over East Asia, real-vector EOF analysis was applied to the vertically integrated water
145 vapor flux anomaly over East Asia-WNP. The principle of the real-vector empirical
146 orthogonal function (R-EOF) technique, applied to two-dimensional vector fields,

¹ <http://jra.kishou.go.jp>

² <http://www.cpc.ncep.noaa.gov>

147 (e.g., $[u;v]$), is presented briefly as follows: first, construct a new $2P \times N$ matrix \mathbf{U} by
 148 adding v to the end of u , that is,

$$149 \quad \mathbf{U} = (u, v) = \begin{bmatrix} u_{11} & u_{12} & \cdots & u_{1N} & v_{11} & v_{12} & \cdots & v_{1N} \\ u_{21} & u_{22} & \cdots & u_{2N} & v_{21} & v_{22} & \cdots & v_{2N} \\ \vdots & \vdots & \ddots & \vdots & \vdots & \vdots & \ddots & \vdots \\ u_{P1} & u_{P2} & \cdots & u_{PN} & v_{P1} & v_{P2} & \cdots & v_{PN} \end{bmatrix}_{2P \times N} .$$

150 where P is the total number of grid points, and N is the total number of time points.
 151 Then calculate the eigenvectors, eigenvalues, and the corresponding principal
 152 components (PCs) of \mathbf{U} using EOF analysis. More details can be found in Kaihatu et
 153 al. (1998) and Marmorino et al. (1999).

154

155 3. Dominant modes of moisture circulation

156 The first two leading modes of the vertically integrated water vapor flux
 157 anomaly over East Asia-WNP (90–150°E, 5–45°N) based on the JRA-25 reanalysis
 158 dataset will be investigated in detail (Fig. 1). They are well separated according to
 159 North et al. (1982). Together, these two modes account for more than 57% of the total
 160 variance and therefore explain a large percentage of the variation in water vapor
 161 transport over East Asia-WNP. To militate against the possible reliance of the EOF
 162 technique on the particular study area and period, as well as the uncertainty within the
 163 dataset, the ECMWF 40 Year Re-analysis (ERA-40) dataset is also applied to the EOF
 164 analysis over the same region, as well as over a larger region, and over an expanded
 165 time period of 1958–2002 (figures not shown). Though focusing on different domains
 166 and time spans, the results based on ECMWF ERA-40 dataset are similar to those in
 167 our study.

168 The first dominant mode (EOF1) captures 43% of the total variance, exhibiting
 169 an extensive anomalous moisture circulation over the WNP. When the corresponding

170 principal component (PC1) is positive, a strong easterly water vapor transport band
171 dominates between around 5–20°N over the WNP. This transport band is separated
172 into two branches to the east of Indochina. One of these continuously transports
173 moisture westward to the northern Indian Ocean, which is the reverse of the
174 climatological moisture transport, indicating that the westerly transport of water vapor
175 to East Asia-WNP by the South Asia summer monsoon flow is weakened. The other
176 branch moves northward over the South China Sea (SCS), bringing abundant
177 moisture to southeastern China, and turns east at around 30°N to the south of Japan. It
178 forms an extensive anticyclonic moisture circulation, elongated along around 20°N
179 over the WNP, enhancing the southeast summer monsoon flow from the WNP to East
180 Asia, that is, the enhanced western North Pacific summer monsoon (WNPSM) flow.
181 Associated with this water vapor transport pattern, anomalous water vapor divergence
182 is found over the SCS and the tropical WNP where the abnormal water vapor
183 originates, while abnormal convergence is located in the mid-latitudes from the
184 Yangtze River valley to the south of Japan, implying the possibly strengthened Mei-
185 Yu/Baiu. The reverse will occur when the PC1 is negative.

186 The principal component of EOF1 shows an obvious interannual variation, with
187 the principal period at around 4 years. It is strongly correlated with the WNPSM
188 index, with a correlation coefficient of -0.97 (> 99% confidence level, figure not
189 shown). This mode thus mainly represents the linkage between anomalous water
190 vapor transport over East Asia-WNP and the intensity of the WNPSM. When the
191 WNPSM is weak, westerly water vapor transport from the Indian summer monsoon
192 region to the WNP is weakened, while more moisture goes northward to South China,
193 resulting in stronger convergence over eastern China and Japan. These results confirm
194 the finding that in weak WNPSM years, the convection along 10–20°N extending

195 from the SCS to the central Pacific is suppressed while rainfall along the Mei-Yu/Baiu
196 front is enhanced (Wang et al. 2001).

197 The second mode (EOF2) accounts for 14% of the total variance. It exhibits a
198 alternating pattern over East Asia-WNP. That is, when PC2 is positive, an anticyclonic
199 moisture circulation anomaly prevails at around 15–30°N, with two cyclonic
200 anomalies lying to its south and north. The anticyclonic moisture circulation in the
201 middle is the strongest and most widespread, with its ridge lying stably at about 25°N,
202 which is near the climatological location of the WPSH ridge (24.3°N). It brings
203 abundant moisture from the subtropical WNP to East Asia, where it meets the
204 cyclonic water vapor transport anomaly from higher latitudes over the lower Yangtze
205 River and Huaihe River valleys, then travels onward to the southern and central
206 portions of Japan. To the south of the anticyclonic moisture circulation, anomalous
207 moisture flow comes from the subtropical WNP, then turns southeastward over the
208 Philippines and moves eastward to the mid-Pacific along the equator, suggesting that
209 moisture transport from the tropical WNP to East Asia is weakened and the abnormal
210 moisture is mainly from the subtropical WNP. The associated water vapor divergence
211 also presents a alternating pattern, with negative-positive-negative anomalies
212 elongating in a zonal direction around 10°N, 20°N, and 30°N, respectively.

213 The principal component of EOF2 (PC2) shows a significant decadal variation,
214 with pronounced interannual change before 1997. This EOF mode reflects the
215 influence of the strength of the WPSH and the southward invasion of cooler air from
216 middle to high latitudes on moisture circulation. When the WPSH is strong, with its
217 ridge stably lying at around 25°N, and the cooler air invades southward with greater
218 frequency, the moisture circulation anomaly over East Asia shows the alternating
219 pattern described above, and vice versa.

220 Generally, moisture circulation over East Asia-WNP exhibits energetic variability.
221 It is dominated jointly by the activity of three Asian summer monsoon systems of
222 comparable strength: the Indian summer monsoon, the WNPSM, and the EASM. The
223 meridional displacement of the WPSH and its strength also make a significant
224 contribution. These results are consistent with previous studies (e.g., Murakami and
225 Matsumoto 1994; Ueda and Yasunari 1996; Chang 2004).

226

227 **4. Moisture circulation and ENSO**

228 a. How does the change in moisture circulation relate to the ENSO cycle?

229 ENSO is widely accepted as one of the most important factors affecting the
230 summer climate over East Asia (e.g., Fu and Teng 1988; Huang and Fu 1996; Huang
231 and Zhang 1997; Wang et al. 2000; Zhou et al. 2008; Li et al. 2010). It is closely
232 related to monsoon activity over East Asia, which carries abundant moisture from
233 remote sources to the rainfall regions. A better understanding of how and to what
234 extent the ENSO cycle influences water vapor transport may give us insight into how
235 it affects the climate of East Asia.

236 To investigate the possible relationship between ENSO and moisture circulation
237 over East Asia-WNP, the SSTA from pre-summer to post-spring were regressed based
238 on the PCs of two dominant modes of summer moisture circulation (Fig. 2 and Fig.
239 3). As shown in Fig. 2, the most remarkable relationship between PC1 and SSTA was
240 the leading positive SSTA and the lagging negative SSTA over the tropical east-
241 central Pacific. From summer (-1) (-1 represents the year before) to winter (-1), the
242 positive SSTA over the tropical east-central Pacific increased, with the amplitude in
243 winter (-1) reaching 0.6°C, doubling that in summer (-1), indicating the development
244 of an El Niño event. These positive SSTA decreased dramatically in the following

245 spring (0) (0 represents the year in which summer moisture circulation is studied) and
246 even turned into a weak negative SSTA in summer (0), revealing the decay of an El
247 Niño event. From autumn (0) to winter (0), the negative SSTA developed rapidly, with
248 the amplitude over -0.8°C over the east-central Pacific, which implied the
249 development of a La Niña event. This negative SSTA persisted even into the spring
250 (+1) (+1 represents the year after). In summary, the positive phase of the first mode of
251 moisture circulation over East Asia-WNP tends to occur in the summer that was
252 preceded by an El Niño event and followed by a La Niña event. That is, when the
253 SSTA over the east-central Pacific shifts from positive to negative, especially during
254 the more pronounced shift from El Niño to La Niña, an abnormal anticyclonic
255 moisture circulation may dominate tropical-subtropical East Asia-WNP. In this case,
256 westerly water vapor transport from the northern Indian Ocean to East Asia-WNP is
257 weakened and more moisture is transferred northward into southeastern China and to
258 the south of Japan, and vice versa.

259 Analysis of the relationship between SSTA and the second mode showed a
260 significant positive SSTA in the tropical east-central Pacific from pre-autumn to post-
261 winter. The positive SSTA developed steadily from autumn (-1) to winter (0), with its
262 center propagating from the central to the eastern Pacific and its amplitude increasing
263 from 0.3°C to 0.5°C . However, in the succeeding spring (+1), the positive SSTA
264 showed obvious decay. Hence, it can be concluded that the positive phase of the
265 second mode of moisture circulation over East Asia-WNP tends to occur in those
266 summers when the positive SSTA over the tropical east-central Pacific develops
267 continuously from the previous year to the succeeding winter. Therefore, in the
268 summers when a low-frequency El Niño event (4-yr period, which will be discussed
269 in following sections) steadily develops, an alternating pattern, that is, an anticyclonic

270 moisture circulation anomaly lying over the subtropical WNP with two cyclonic
271 anomalies to its south and north, may exist. In this case, the moisture transport over
272 East Asia from the subtropical WNP is enhanced, while that from the tropical WNP is
273 decreased. The opposite may happen in the case of a low-frequency La Niña event.

274 To verify these results, the relationship between ENSO and moisture circulation
275 over East Asia-WNP was further investigated by analyzing the extreme cases. These
276 cases were selected based on their PC values (greater/less than one standard deviation,
277 Table 1). In seven cases with extreme positive PC1, six cases occurred in summers
278 that were preceded by positive SSTA and followed by negative SSTA in the Niño 3
279 region; even more notable, four cases occurred in the summers preceded by El Niño
280 and followed by La Niña events. In the case of extreme negative PC1, four out of six
281 cases took place in summers which were preceded by negative SSTA and followed by
282 positive SSTA in the Niño 3 region. For the positive/negative PC2, three out of four
283 extreme cases occurred in summers when El Niño/La Niña events developed
284 continuously. The distribution of composite tropical SSTA patterns from Jan (-2, two
285 years before) to Dec (+2, two years after), based on the extreme years defined in
286 Table 1, is also investigated (Fig. 4). Locked phase relationships between SSTA over
287 the east-central Pacific and the first two leading modes of moisture circulation were
288 also found in the composite study, which is consistent with the result from the
289 regression study. Furthermore, a comparison of Fig. 4a and 4b demonstrates that these
290 locked phase relationships do not develop independently but construct a quasi-four-
291 year coupling. That is, during a quasi-four-year periodic ENSO cycle, when the warm
292 episode is developing continually, the positive phase of the second mode tends to play
293 a key role in the moisture circulation anomaly over East Asia-WNP; in the transitional
294 summer between a decaying warm phase and a developing cool phase, the positive

295 phase of the first mode tends to take effect; during the summer of a developing cool
296 episode, the negative phase of the second mode tends to play an important role; and
297 the negative phase of the first mode tends to take effect in the transitional summer of a
298 decaying cool episode and a developing warm episode.

299

300 b. Why does the ENSO cycle affect moisture circulation over East Asia?

301 As discussed above, the SSTA over the east-central Pacific couples well with the
302 moisture circulation over East Asia-WNP during the quasi-four-year ENSO period. To
303 support our argument, the possible teleconnection within this quasi-four-year coupling
304 will be illustrated by regressing the SSTA and lower atmospheric circulation based on
305 the PCs of two leading modes of moisture circulation (Fig. 5). The lower atmospheric
306 circulation is selected for regression considering that the wind field not only can
307 represent the response of the atmosphere to the SSTA, but also can reflect the
308 vertically integrated water vapor transport as most of the moisture is concentrated on
309 the lower level. It is interesting to note that from Fig. 5f–j to Fig. 5a–e and to the
310 opposite sign of Fig. 5f, and so on, the regressed SSTA and atmospheric circulation
311 form a quasi-four-year cycle. Furthermore, these regressed circulation patterns,
312 especially the zonal wind anomalies over the tropical Pacific, couple well with the
313 development of the quasi-four-year ENSO episodes.

314 As shown in Fig. 5g, the regressed 850-hPa wind circulation over East Asia-WNP
315 shows an alternating pattern with an anticyclone over the subtropical WNP and two
316 cyclonic circulations to its south and north, which is exactly the same as the pattern of
317 the positive phase of the second mode of moisture circulation. It should be
318 emphasized that to the south of the southern cyclonic circulation, a strong westerly
319 wind anomaly prevails over the tropical west-central Pacific. This westerly wind

320 anomaly propagates farther eastward to the eastern Pacific in the following autumn
321 and winter, implying that the equatorial easterlies over the Pacific are weakened in the
322 lower atmosphere. This is beneficial to the formation and eastward propagation of a
323 warm Kelvin wave. This eastward propagation can initiate the westerly transportation
324 of warm water from the western Pacific warm pool to the eastern Pacific and cause
325 the continuous development of an El Niño event (Huang et al. 2004). Meanwhile, an
326 anticyclonic circulation forms abruptly over the Philippine Sea during the following
327 winter (Fig. 5i), which is termed the Philippine Sea Anticyclone (PSAC; Wang et al.
328 2000). The PSAC, persisting from the mature phase of El Niño until the ensuing
329 summer, plays a vital role in the teleconnection between ENSO events and the climate
330 of East Asia (Wang et al. 2000, Zhou et al. 2009b; Li and Yang 2010). It undergoes an
331 eastward shift in the succeeding seasons (Wang and Zhang 2002; Lau and Weng
332 2002) and develops into a strong anticyclonic circulation over the tropical-subtropical
333 WNP (Fig. 5b), which is identical to the pattern of moisture circulation shown in the
334 positive phase of the first mode. Associated with the establishment and eastward
335 extension of the PSAC, an easterly wind anomaly starts to prevail over the maritime
336 continental region and then stretches to the central Pacific in the east, and to the Bay
337 of Bengal in the west. This easterly wind anomaly is favorable for the formation and
338 eastward propagation of a cold Kelvin wave in the western Pacific warm pool (Huang
339 et al. 2004). Therefore, this strong easterly wind band not only ushers in the
340 weakening of the WNPSM and the reduction in water vapor transported from the
341 Indian monsoon region to the WNP, but also results in the disappearance of an El
342 Niño event and the establishment of a La Niña event. During the next autumn and
343 winter (Fig. 5c and 5d), along with the sustainable extension of the easterly wind to
344 the east, the cooling effect on the Niño region strengthens. At the same time, the

345 PSAC shifts eastward to the east of the Philippine Sea; a cyclonic circulation first
346 forms over the north of South China Sea, then strongly develops northeastward and
347 replaces the anticyclone, dominating a large area of the WNP during the following
348 spring (Fig. 5e). Figures 5f and 5e show nearly the same pattern, but with the opposite
349 sign. Thus, the opposite phase of the quasi-four-year coupling between ENSO and the
350 two dominant modes of moisture circulation over East Asia-WNP can be illustrated
351 by reversing the sign of the patterns shown in Fig. 5. That is, the negative phase of the
352 second mode tends to play an important role during the summer of a developing cool
353 episode (the opposite of Fig. 5g), and the negative phase of the first mode tends to
354 take effect in the transitional summer of a decaying cool episode and a developing
355 warm episode (the opposite of Fig. 5a). Hence, the quasi-four-year coupling between
356 ENSO and water vapor transport over East Asia-WNP is convincing, and the
357 anticyclone/cyclone over the Philippine Sea region plays an important role in this
358 quasi-four-year coupling.

359

360 **5. Case study**

361 In this section, further examination of the quasi-four-year coupling between
362 ENSO and water vapor transport over East Asia-WNP is carried out by analyzing the
363 cases in observation. The annual distribution of the primary EOF mode of moisture
364 circulation over East Asia-WNP (the mode that accounts for the largest percent of the
365 total variance) is shown in Fig. 6. The evolution of the primary EOF mode during
366 1983–1984 is from the positive phase of the first mode to the negative phase of the
367 second mode. During 1986–1990, it is from the negative phase of the first mode to the
368 positive phase of the second mode, to the positive phase of the first mode, and to the
369 negative phase of the second mode. During 2002–2003, it is from the negative phase

370 of the first mode to the positive phase of the second mode. Comparing these with the
371 evolution of the EOF modes in the quasi-four-year coupling, it can be stated that the
372 years 1983–1984, 1986–1990, and 2002–2003 match the quasi-four-year coupling.
373 We therefore selected the years 1983–1984 and 1986–1987 for detailed analysis in the
374 following study.

375

376 a. Water vapor transport during 1983–1984

377 The SSTA over the Niño 3 region shifted from strongly above normal to weakly
378 below normal in 1983 and remained below normal in 1984 (Fig. 7a). Hence, the
379 summer of 1983 was the transitional summer between a decaying warm phase and a
380 developing cool phase of an ENSO episode, when the positive phase of the first mode
381 tends to play a key role in moisture circulation according to the quasi-four-year
382 coupling. On the other hand, the summer of 1984 was the summer of a steadily
383 developing cool phase, when the negative phase of the second mode tends to take
384 effect. These can be verified by noting the water vapor transport anomaly patterns in
385 the summers of 1983 and 1984, which are shown in Fig. 7b and 7c. In Fig. 7b, it can
386 be found that an extensive anticyclonic moisture circulation dominated the tropical
387 and subtropical WNP-East Asia and a vast band of easterly zonal transport anomaly
388 over the tropical WNP and the Bay of Bengal. This is nearly identical to the spatial
389 distribution of the positive phase of the first mode shown in Fig. 1a. In Fig. 7c, a
390 strong cyclonic moisture circulation anomaly prevails in the subtropical WNP, with
391 two anticyclonic anomalies lying to its south and north, which is the exact opposite of
392 the pattern shown in Fig. 1b, indicating that the negative phase of the second mode
393 played an important role in the summer of 1984.

394

395 b. Water vapor transport during 1986–1987

396 The SSTA over the Niño 3 region shifted from below normal to above normal in
397 the spring of 1986, and positive SSTA developed continually during the second half of
398 1986 and all through 1987 (Fig. 8a). Hence, the summer of 1986 was the transitional
399 summer between a decaying La Niña and a developing El Niño event, when the
400 negative phase of the first mode tends to play a key role in the moisture circulation
401 according to the quasi-four-year coupling described in the last section. On the other
402 hand, the summer of 1987 was the developing summer of an El Niño event, when the
403 positive phase of the second mode should take effect. Similarly, this can be confirmed
404 by the abnormal summer moisture circulation in 1986 and 1987, as shown in Fig. 8b
405 and 8c.

406 Hence, the quasi-four-year coupling between SSTA over the east-central Pacific
407 and moisture circulation over East Asia-WNP can be confirmed by these cases
408 studies.

409

410 **6. Summary**

411 Summer moisture circulation over East Asia-WNP exhibits an energetic annual
412 variation. To study its spatial and temporal distribution, the R-EOF technique was
413 applied to the vertically integrated water vapor fluxes. It was found that moisture
414 circulation over East Asia-WNP is dominated primarily by two well-separated modes.
415 These two modes couple well with the low-frequency ENSO during its quasi-four-
416 year cycle. Further study showed that the anticyclone (cyclone) over the Philippine
417 Sea and the easterly (westerly) wind anomaly to its south play an important role in
418 maintaining this quasi-four-year coupling. The main results are summarized below.

419 Moisture circulation over East Asia is dominated by two well-separated modes.

420 One exhibits an anomalous anticyclonic (cyclonic) moisture circulation over the
421 tropical-subtropical WNP and an easterly (westerly) transport anomaly over the
422 tropical Indian Ocean and WNP. This is tightly connected to the weaker (stronger)
423 WNPSM. The second mode exhibits an alternating pattern, with an anticyclonic
424 (cyclonic) moisture circulation anomaly over the subtropical WNP and two cyclonic
425 (anticyclonic) anomalies to its south and north. This mode is closely associated with
426 the strength of the WPSH.

427 These two dominant modes of moisture circulation closely relate to the leading
428 and lagging SSTA over the tropical east-central Pacific. A quasi-four-year coupling
429 between moisture circulation over East Asia and the ENSO signal was found. That is,
430 during the quasi-four-year ENSO cycle, the positive phase of the second mode tends
431 to take effect when a warm episode is developing continually, while the positive phase
432 of the first mode tends to play a key role in the transitional summer between a
433 decaying warm phase and a developing cool phase. In the summer of a developing
434 cool episode, the negative phase of the second mode tends to take effect, while the
435 negative phase of the first mode tends to play an important role in the transitional
436 summer between a decaying cool episode and a developing warm episode.

437 The anticyclone (cyclone) over the Philippine Sea region serves as a bridge
438 between moisture circulation over East Asia-WNP and ENSO events in the quasi-
439 four-year coupling. Its establishment in the mature phase and eastward extension in
440 the following phase of the warming (cooling) episode play an important role in the
441 variation of moisture circulation over East Asia-WNP. Conversely, the easterly
442 (westerly) wind anomaly to the south of the anticyclone (cyclone) is favorable for the
443 formation and eastward propagation of a cold (warm) Kelvin wave, hence stimulating
444 the development of the warming (cooling) episodes associated with the ENSO cycle.

445 However, as shown in section 5, examples of perfect quasi-four-year coupling are
446 limited in the observation. This may be due to the rarity of the self-contained quasi-
447 four-year cycle ENSO events. Jiang et al. (1995) concluded that multiple time scale
448 oscillations may be involved in the ENSO variability. In addition to the quasi-four-
449 year period mentioned above, the spectral peaks at 28, 24, and 15 months are also
450 major modes of interannual variability of the ENSO events; within these, the 28-
451 month oscillation is statistically significant in all cases and, if combined with the 24-
452 month oscillation, could be as robust as the 4-year mode. What is more, the 15-month
453 mode may interact with the 4-year cycle nonlinearly. Therefore, the quasi-four-year
454 coupling of moisture transport over East Asia-WNP and ENSO events may be
455 disturbed by other modes of the ENSO signal, which may be the reason for the
456 limited number of observed examples of perfect quasi-four-year couplings. However,
457 this hypothesis needs further testing.

458 The southwest flow of the Indian summer monsoon, which brings abundant
459 evaporated moisture from the Indian Ocean, is one of three important branches of
460 water vapor transport over East Asia (Li et al. 2011). It is not surprising that in
461 addition to the SSTAs over the tropical east-central Pacific, the thermal state of the
462 Indian Ocean may also play a vital role in modifying moisture transport over East
463 Asia-WNP. Previous studies have noted that the Indian Ocean SSTA that developed in
464 response to both atmospheric and oceanic processes of ENSO events need to be
465 considered for a complete understanding of regional climate variability. The SSTA
466 over the Indian Ocean may contribute to the development of a low-level anticyclone
467 (cyclone) over the Philippines via its adjustment in the Walker circulation (Annamalai
468 et al. 2005; Yuan et al. 2008) and via the Kelvin wave–induced Ekman divergence
469 mechanism (Xie et al. 2009). Furthermore, the anomalous heating (cooling) over the

470 north Indian Ocean can decrease (increase) the north-south heating gradient, which is
471 favorable for a weak (strong) Indian summer monsoon flow and thus leads to weak
472 (strong) water vapor transport (Zhang 2001). Zhang also found that the weaker
473 (stronger) the Indian summer monsoon water vapor transportation is, the stronger
474 (weaker) the WPSH becomes in its southwestern portion, which leads to more (less)
475 water vapor transport to East Asia (refer to Fig. 3 in Zhang 2001). This is exactly the
476 pattern of abnormal water vapor transport in the first mode described in section 3. As
477 we can see in Fig. 3e, the regression of SSTA over the northern Indian Ocean based
478 on PC1 is significantly positive, indicating that the first mode of summer moisture
479 circulation over East Asia-WNP closely relates to the concurrent SSTA over the
480 northern Indian Ocean. It should be pointed out that the second mode significantly
481 correlates with the SSTA over the Indian Ocean too. However, the correlated SSTA
482 initially exists over the tropical eastern Indian Ocean in the previous spring and
483 persists until the summer, with its strength slightly weakened but its location
484 expanded to include the whole north Indian Ocean. Hence, the two dominant patterns
485 of water vapor transport over East Asia-WNP couple with not only the SSTA over the
486 east-central Pacific, but also the SSTA over the Indian Ocean. Unlike the first mode,
487 which is closely related only to the simultaneous SSTA over the north Indian Ocean,
488 the second mode is also related to the SSTA over the eastern Indian Ocean in the
489 previous spring. It seems that the difference in the time span of abnormal heating over
490 the Indian Ocean may lead to different effects on the moisture circulation over East
491 Asia-WNP. This needs further examination in a future study.

492 In this study, we focused on the coupling between water vapor transport over East
493 Asia-WNP and warming events over the East Pacific and pointed out that the
494 development of the PSAC during different phases of the warming events played an

495 important role in this coupling. However, recent studies have shown that there are two
496 different types of warming events over the Pacific Ocean, El Niño and El Niño
497 Modoki, the impacts of which are significantly different on atmospheric circulation
498 and precipitation over East Asia. In particular, these differences are attributed mainly
499 to the discrepancy in the evolution and location of the PSAC and WPSH associated
500 with the two types of events. In comparison of the major El Niño Modoki events
501 defined by Feng et al. (2010) with the cases that obey the quasi-four-year coupling
502 described in section 5, 2002–2003 is found to be an El Niño Modoki event and obeys
503 the quasi-four-year coupling. It seems that both El Niño and El Niño Modoki events
504 could couple with water vapor transport over East Asia-WNP in a quasi-four-year
505 cycle. Hence, it is necessary to study in detail the different roles played by the two
506 types of warming events in our quasi-four-year coupling in a future study.

507

508 *Acknowledgments:* This research is supported by 973 Basic Research Program Grant
509 (2009CB4214404), Joint National Natural Science Foundation of China Project (U0733002),
510 and the City University of Hong Kong Strategic Research Grants (7002505).

511 REFERENCES:

- 512 Annamalai, H., P. Liu, and S. P. Xie, 2005: Southwest Indian Ocean SST variability: Its local
513 effect and remote influence on Asian monsoon. *J. Climate*, **18**, 4150–4167.
- 514 Benton, G. S., R. T. Blackburn, and V. O. Snead, 1950: The role of the atmosphere in the
515 hydrologic cycle. *Eos Transactions AGU*, **31**, 61–73.
- 516 Budyko, M. I., 1974: *Climate and life* (Internal Geophysics Series). Academic Press, 508 pp.
- 517 Chang, C. P., 2004: *The East Asian monsoon*. World Scientific Publishing Company, 564 pp.
- 518 Chen, L. X., M. Dong, and Y. N. Shao, 1992: The characteristics of interannual variations on
519 the East Asian monsoon. *J. Meteorol. Soc. Japan*, **70**, 397–421.
- 520 Chen, W., 2002: The impacts of El-Niño and La-Niña on the cycle of East Asian winter and
521 summer monsoon. *Chin. J. Atmos. Sci.*, **01**, 1–12 (in Chinese).
- 522 Climate Prediction Center (2005-12-19). “ENSO FAQ: How often do El-Niño and La-Niña
523 typically occur?” National Centers for Environmental Prediction. Retrieved 2009-07-26.
- 524 Ding, Y. H., 1992: Summer monsoon rainfalls in China. *J. Meteorol. Soc. Japan*, **70**, 373–
525 396.
- 526 Feng, J., L. Wang, W. Chen, S. K. Fong, and K. C. Leong, 2010: Different impacts of two
527 types of Pacific Ocean warming on Southeast Asian rainfall during boreal winter, *J.*
528 *Geophys. Res.*, **115**, D24122, DOI: 10.1029/2010JD014761.
- 529 Feng, J., W. Chen, C. Y. Tam, and W. Zhou, 2011: Different impacts of El Niño and El Niño
530 Modoki on China rainfall in the decaying phases. *Int. J. Climatol.*, **31**, 2091–2101.
- 531 Fu, C. B., and X. L. Teng, 1988: Climate anomalies in China associated with El-
532 Niño/Southern Oscillation. *Chin. J. Atmos. Sci.*, **12S**, 133–141 (in Chinese).
- 533 Hattori, M., K. Tsuboki, and T. Takeda, 2005: Interannual variation of seasonal changes of
534 precipitation and moisture transport in the western North Pacific. *J. Meteorol. Soc.*
535 *Japan*, **83**, 107–127.
- 536 Huang, R. H., W. Chen, B. L. Yan, and R. H. Zhang, 2004: Recent advances in studies of the
537 interaction between the East Asian winter and summer monsoons and ENSO cycle. *Adv.*
538 *Atmos. Sci.*, **21**, 407–424.

- 539 —, and Y. F. Fu, 1996: The interaction between the East Asian monsoon and ENSO cycle.
540 *Climatic Environ. Res.*, **01**, 38–54 (in Chinese).
- 541 —, and Y. F. Wu, 1989: The influence of ENSO on the summer climate change in China
542 and its mechanisms. *Adv. Atmos. Sci.*, **06**, 21–32.
- 543 —, and R. H. Zhang, 1997: Diagnostic study on the interaction between ENSO cycle and
544 East Asian monsoon circulation. *Memorial Papers to Prof. Zhao Jiuzhang*, D. Z. Ye, Ed.,
545 China Science Press, 93–109.
- 546 —, and L. T. Zhou, 2002: Research on the characteristics, formation mechanism and
547 prediction of severe climate disasters in China. *J. Nat. Disasters*, **11**, 1–9 (in Chinese).
- 548 Jiang, N., J. D. Neelin, and M. Ghil, 1995: Quasi-quadrennial and quasi-biennial variability in
549 the equatorial Pacific. *Clim. Dynam.*, **12**, 101–112.
- 550 Kaihatu, J. M., R. A. Handler, G. O. Marmorino, and L. K. Shay, 1998: Empirical orthogonal
551 function analysis of ocean surface currents using complex and real-vector methods. *J.*
552 *Atmos. Ocean. Tech.*, **15**, 927–941.
- 553 Kripalani, R. H., and A. Kulkarni, 2001: Monsoon rainfall variations and teleconnections over
554 South and East Asia. *Int. J. Climatol.*, **21**, 603–616.
- 555 Lau, K. M., and H. Weng, 2002: Recurrent teleconnection patterns linking summertime
556 precipitation variability over East Asia and North America. *J. Meteorol. Soc. Japan*, **80**,
557 1129–1147.
- 558 Li, J. P., Z. W. Wu, Z. H. Jiang, and J. H. He, 2010: Can global warming strengthen the East
559 Asian summer monsoon? *J. Climate*, **23**, 6696–6705.
- 560 Li, X. Z., Z. P. Wen, and W. Zhou, 2011: Long-term changes in summer water vapor transport
561 over South China in recent decades. *J. Meteorol. Soc. Japan*, **89A**, 271–282.
- 562 Li, Y. Q., and S. Yang, 2010: A dynamical index for the East Asian winter monsoon. *J.*
563 *Climate*, **23**, 4255–4262.
- 564 Macmynowski, D. G., and E. Tziperman, 2008: Factors affecting ENSO's period. *J. Atmos.*
565 *Sci.*, **65**, 1570–1586.
- 566 Marmorino, G. O., L. K. Shary, B. K. Haus, R. A. Handler, H. C. Graber, and M. P. Horne,

567 1999: An EOF analysis of HF Doppler radar current measurements of the Chesapeake
568 Bay buoyant outflow. *Continent. Shelf Res.*, **19**, 271–288.

569 Murakami, T., and J. Matsumoto, 1994: Summer monsoon over the Asian continent and
570 western North Pacific. *J. Meteorol. Soc. Japan*, **70**, 597–611.

571 North, G. R., T. L. Bell, and R. F. Cahalan, 1982: Sampling errors in the estimation of
572 empirical orthogonal functions. *Mon. Weather Rev.*, **110**, 699–706.

573 Onogi, K. J. T., H. Koide, M. Sakamoto, S. Kobayashi, H. Hatsushika, T. Matsumoto, N.
574 Yamazaki, H. Kamahori, K. Takahashi, S. Kadokura, K. Wada, K. Kato, R. Oyama, T.
575 Ose, N. Mannoji, and R. Taira, 2007: The JRA-25 reanalysis. *J. Meteorol. Soc. Japan*, **85**,
576 369–432.

577 Rasmusson, E. M., X. Wang, and C. F. Ropelewski, 1990: The biennial component of ENSO
578 variability. *J. Mar. Syst.*, **01**, 71–96.

579 Ropelewski, C. F., M. S. Halpert, and X. Wang, 1992: Observed tropospheric biennial
580 variability in the global tropics. *J. Climate*, **05**, 594–614.

581 Simmonds, I., D. Bi, and P. Hope, 1999: Atmospheric water vapor flux and its association
582 with rainfall over China in summer. *J. Climate*, **12**, 1353–1367.

583 Smith, T. M., R. W. Reynolds, T. C. Peterson, and J. Lawrimore, 2008: Improvements to
584 NOAA’s historical merged land-ocean surface temperature analysis (1880–2006). *J.*
585 *Climate*, **21**, 2283–2296.

586 Ueda, H., and T. Yasunari, 1996: Maturing process of summer monsoon over the western
587 North Pacific—a couple ocean/atmosphere system. *J. Meteorol. Soc. Japan*, **74**, 493–508.

588 Wang, B., R. G. Wu, and X. H. Fu, 2000: Pacific–East Asian teleconnection: How does ENSO
589 affect East Asian climate? *J. Climate*, **13**, 1517–1536.

590 ———, R. G. Wu, and K. M. Lau, 2001: Interannual variability of Asian summer monsoon:
591 Contrast between the Indian and western North Pacific–East Asian monsoons. *J. Climate*,
592 **14**, 4073–4090.

593 ———, Z. W. Wu, J. P. Li, J. Liu, C. P. Chang, Y. H. Ding, and G. X. Wu, 2008: How to
594 measure the strength of the East Asian summer monsoon. *J. Climate*, **21**, 4449–4463.

595 ———, and Q. Zhang, 2002: Pacific-East Asian teleconnection. Part II: How the Philippine Sea
596 anticyclone established during development of El-Niño. *J. Climate*, **15**, 3252–3265.

597 Xie, S. P., K. Hu, J. Hafner, H. Tokinaga, Y. Du, G. Huang, and T. Sampe, 2009: Indian Ocean
598 capacitor effect on Indo-western Pacific Climate during the summer following El Nino. *J.*
599 *Climate*, **22**, 730–747.

600 Yang, S., K. M. Lau, S. H. Yoo, J. L. Kinter, K. Miyakoda, and C. H. Ho, 2004: Upstream
601 subtropical signals preceding the Asian summer monsoon circulation. *J. Climate*, **17**,
602 4213–4229.

603 Yuan, Y., W. Zhou, J. C. L. Chan, and C. Y. Li, 2008: Impacts of the basin-
604 wide Indian Ocean SSTA on the South China Sea summer monsoon onset. *Int. J.*
605 *Climatol.*, **28**, 1579–1587.

606 Zhang, R. H., 2001: Relations of water vapor transport from Indian monsoon with that over
607 East Asia and the summer rainfall in China. *Adv. Atmos. Sci.*, **18**, 1005–1017.

608 ———, A. Sumi, and M. Kimoto, 1996: Impact of El-Niño on the East Asian monsoon: A
609 diagnostic study of the 86/87 and 91/92 events. *J. Meteorol. Soc. Japan*, **74**, 49–62.

610 Zhou, T. J., and R. C. Yu, 2005: Atmospheric water vapor transport associated with typical
611 anomalous summer rainfall patterns in China. *J. Geophys. Res.*, **110**, D08104, DOI:
612 10.1029/2004JD005413.

613 ———, R. C. Yu, H. M. Li, and B. Wang, 2008: Ocean forcing to changes in global monsoon
614 precipitation over the recent half-century. *J. Climate*, **21**, 3833–3852.

615 ———, R. C. Yu, J. Zhang, H. Drange, C. Cassou, C. Deser, D. L. R. Hodson, E. S. Gomez, J.
616 Li, N. Keenlyside, X. G. Xin, and Y. Okumura, 2009a: Why the western Pacific
617 subtropical high has extended westward since the late 1970s. *J. Climate*, **22**, 2199–2215.

618 Zhou, W., J. C. L. Chan, W. Chen, J. Ling, J. G. Pinto, and Y. P. Shao, 2009b: Synoptic-scale
619 controls of persistent low temperature and icy weather over southern China in January
620 2008. *Mon. Weather Rev.*, **137**, 3978–3991.

621 **Catalog of graphs:**

622 Fig. 1. Spatial and temporal distribution for EOFs of summer water vapor flux anomalies over
623 East Asia-WNP during 1979–2009. (a) EOF1 and (b) EOF2. Figures in the upper panel
624 are the eigenvectors, unit: $\text{kg m}^{-1} \text{s}^{-1}$; figures in the lower panel are the associated
625 principal components (PCs). The shading in the upper panel represents the associated
626 divergence of water vapor fluxes over $8 \times 10^{-6} \text{ kg m}^{-2} \text{ s}^{-1}$ (light gray) and less than -
627 $8 \times 10^{-6} \text{ kg m}^{-2} \text{ s}^{-1}$ (dark gray). The dashed lines in the lower panel indicate $\pm \sigma$ of PCs.

628 Fig. 2. Regression of seasonal sea surface temperature anomalies (SSTAs) based on the time
629 coefficient of EOF1 (PC1) of summer moisture circulation over East Asia-WNP from
630 pre-summer to post-spring. Unit: K. Shaded areas indicate regions where the
631 regressions of SSTA are statistically significant at the 95% confidence level by a t-test.
632 (a–h) presents pre-summer to post-spring, respectively. (-1) indicates the year before,
633 (+1) indicates the year after, and (0) indicates the year in which summer moisture
634 circulation is studied.

635 Fig. 3. Same as Fig. 2, but based on the PC2.

636 Fig. 4. Distribution of composite positive-minus-negative anomaly patterns of tropical (-
637 $5 \sim 5^\circ\text{N}$ averaged) SST from two years before to two years after based on the extreme
638 years selected based on the (a) PC1 and (b) PC2. Unit: K. -2, -1, 0, +1, and +2
639 represent two years before, the year before, the year when summer moisture
640 circulation is studied, the year after, and two years after, respectively.

641 Fig. 5. Regression of the lower-troposphere wind field (unit: m s^{-1}) and SSTA (unit: K) from
642 pre-spring (spring [0]) to post-spring (spring [+1]) based on PC1 and PC2,
643 respectively. Only those with regressed wind speed over 0.2 m s^{-1} are displaced. The
644 shaded areas indicate regions where the regression is statistically significant at the
645 95% confidence level by a t-test. The contours indicate the regressed SSTA, with the
646 interval of 0.2 K. (a) through (e) are based on PC1, and (f) through (j) are based on

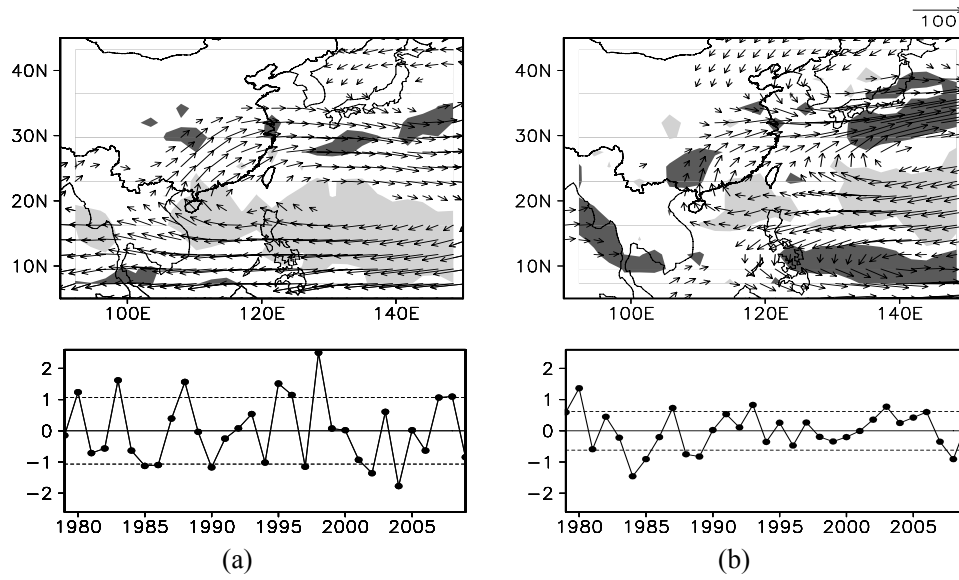
647 PC2.

648 Fig. 6. Annual distribution of the primary EOF mode of moisture circulation over East Asia-
649 WNP (bar, axis on the right) and monthly distribution of SSTA over the Niño 3 region
650 (contour, axis on the left, unit: K) from 1979–2009. The primary EOF mode is decided
651 by ranging the time coefficient of EOF mode 1 to mode 5; the maximum is then
652 considered to be the primary EOF mode; a value > 0 indicates the positive phase of the
653 EOF mode, and a value < 0 indicates the negative phase of the EOF mode.

654 Fig. 7. (a) Time series of monthly SSTA anomalies over the Niño 3 region (unit: K) during
655 Jan 1983 to Dec 1984. Abnormal water vapor transport over East Asia-WNP in the
656 summer of (b) 1983, and (c) 1984.

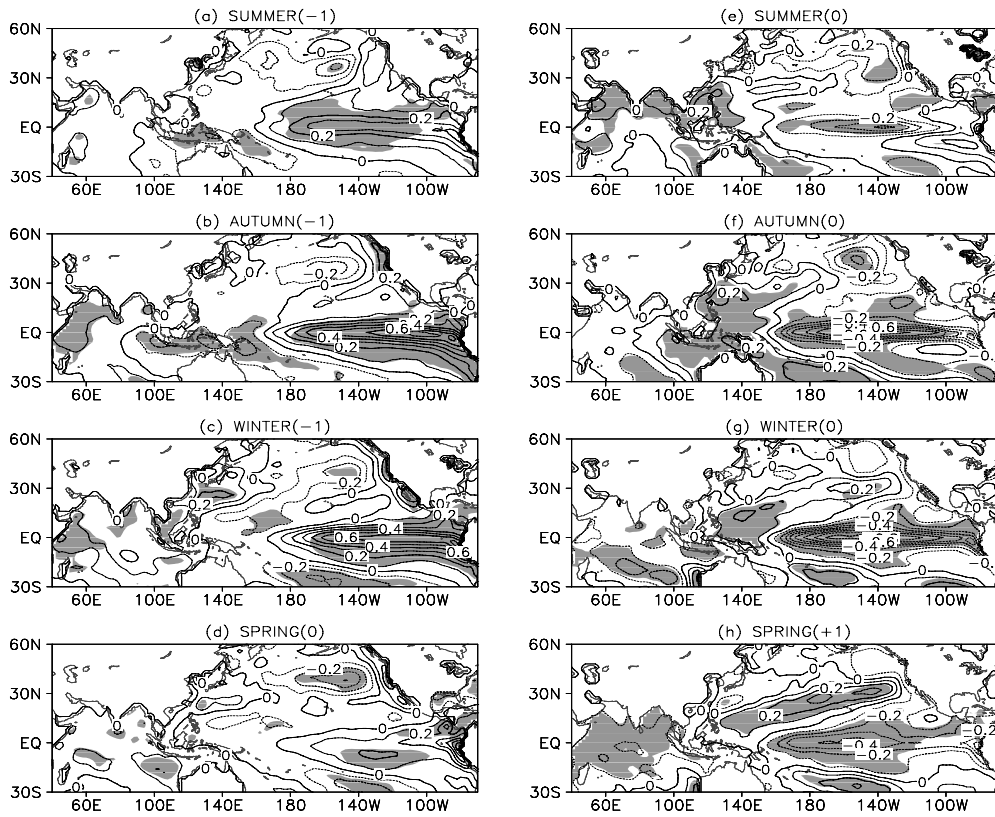
657 Fig. 8. Same as Fig. 7, but for the period of Jan 1986–Dec 1987.

658 Table 1. Extreme years selected based on the PC1 and PC2 (greater/less than one standard
659 deviation), and their relationship with the SSTA over the tropical east-central Pacific.



661

662 Fig. 1. Spatial and temporal distribution for EOFs of summer water vapor flux anomalies over
 663 East Asia-WNP during 1979–2009. (a) EOF1 and (b) EOF2. Figures in the upper panel
 664 are the eigenvectors, unit: $\text{kg m}^{-1} \text{s}^{-1}$; figures in the lower panel are the associated
 665 principal components (PCs). The shading in the upper panel represents the associated
 666 divergence of water vapor fluxes over $8 \times 10^{-6} \text{ kg m}^{-2} \text{ s}^{-1}$ (light gray) and less than -
 667 $8 \times 10^{-6} \text{ kg m}^{-2} \text{ s}^{-1}$ (dark gray). The dashed lines in the lower panel indicate $\pm \sigma$ of PCs.



669

670

671

672

673

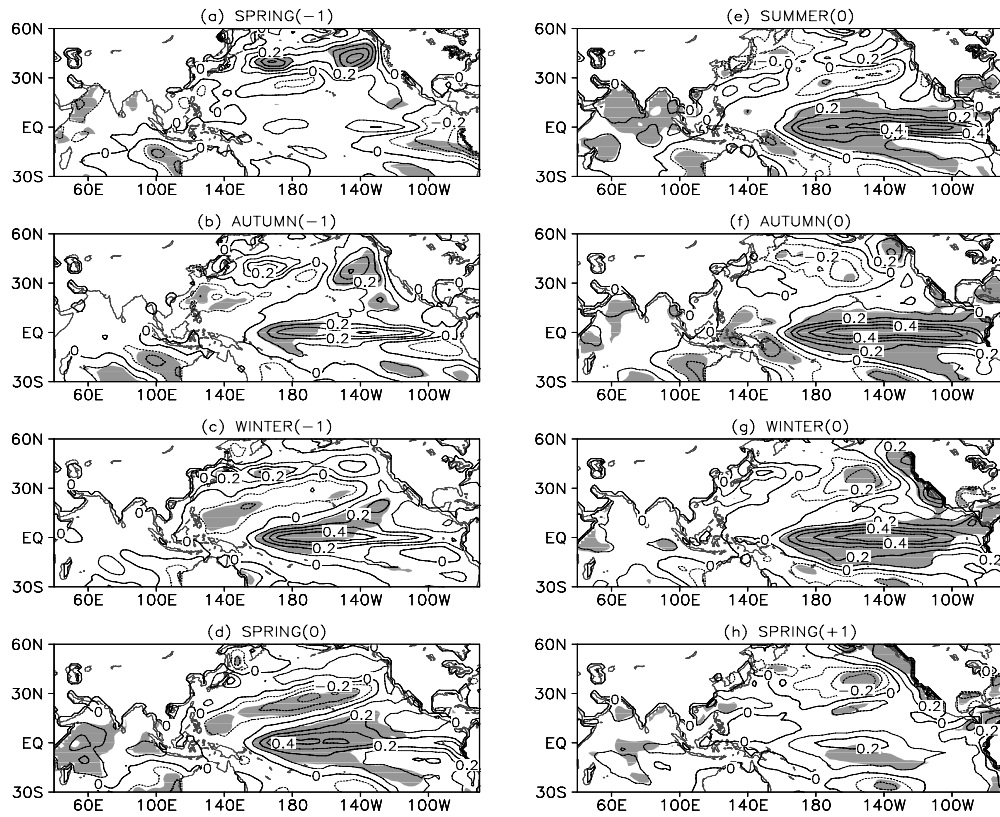
674

675

676

Fig. 2. Regression of seasonal sea surface temperature anomalies (SSTAs) based on the time coefficient of EOF1 (PC1) of summer moisture circulation over East Asia-WNP from pre-summer to post-spring. Unit: K. Shaded areas indicate regions where the regressions of SSTA are statistically significant at the 95% confidence level by a t-test. (a–h) presents pre-summer to post-spring, respectively. (-1) indicates the year before, (+1) indicates the year after, and (0) indicates the year in which summer moisture circulation is studied.

677



678

679 Fig. 3. Same as Fig. 2, but based on the PC2.

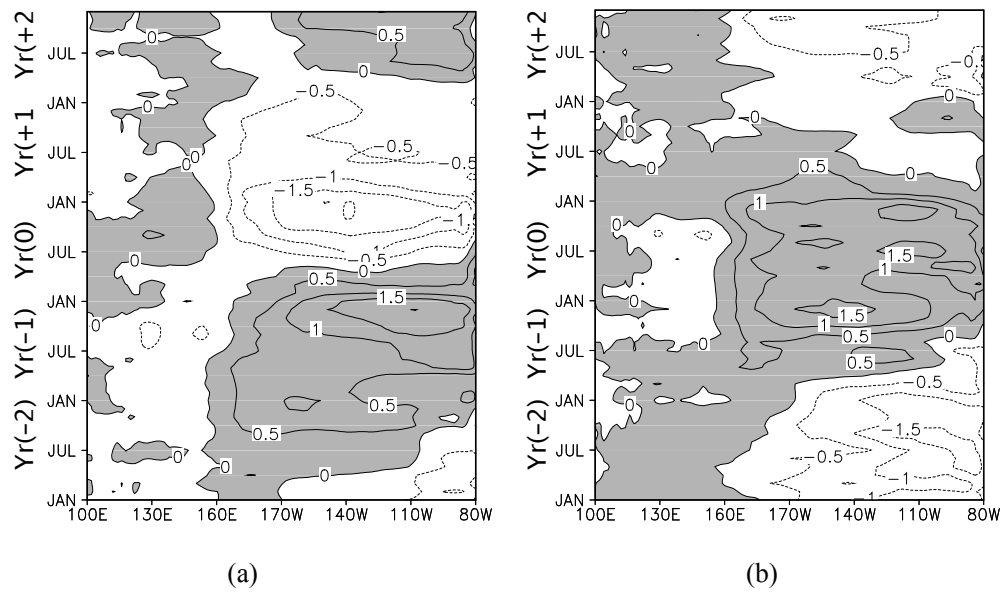
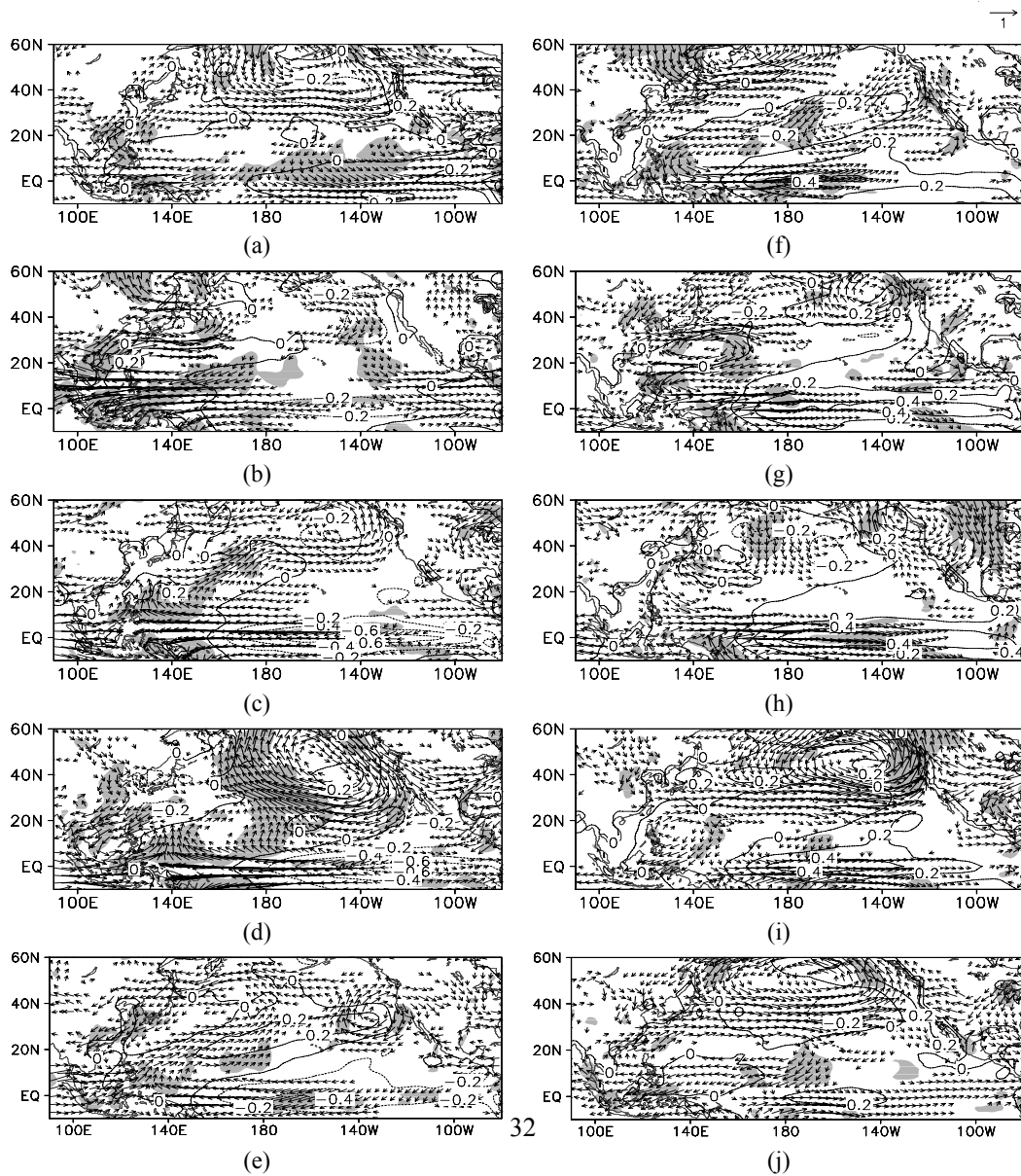


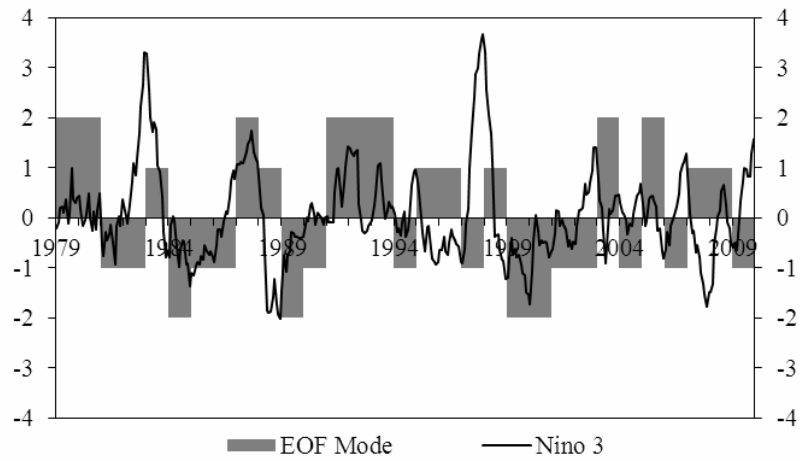
Fig. 4. Distribution of composite positive-minus-negative anomaly patterns of tropical ($-5\sim 5^{\circ}\text{N}$ averaged) SST from two years before to two years after based on the extreme years selected based on the (a) PC1 and (b) PC2. Unit: K. -2, -1, 0, +1, and +2 represent two years before, the year before, the year when summer moisture circulation is studied, the year after, and two years after, respectively.



687

688 Fig. 5. Regression of the lower-troposphere wind field (unit: m s^{-1}) and SSTA (unit: K) from
 689 pre-spring (spring [0]) to post-spring (spring [+1]) based on PC1 and PC2,
 690 respectively. Only those with regressed wind speed over 0.2 m s^{-1} are displaced. The
 691 shaded areas indicate regions where the regression is statistically significant at the
 692 95% confidence level by a t-test. The contours indicate the regressed SSTA, with the
 693 interval of 0.2 K. (a) through (e) are based on PC1, and (f) through (j) are based on
 694 PC2.

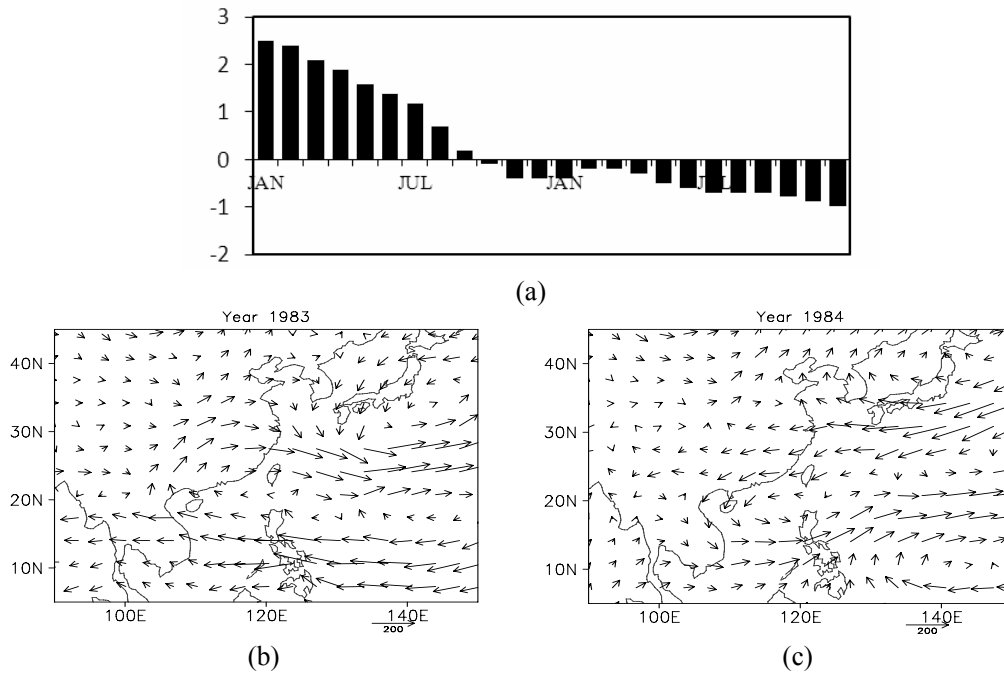
695



696

697 Fig. 6. Annual distribution of the primary EOF mode of moisture circulation over East Asia-
698 WNP (bar, axis on the right) and monthly distribution of SSTA over the Niño 3 region
699 (contour, axis on the left, unit: K) from 1979–2009. The primary EOF mode is decided
700 by ranging the time coefficient of EOF mode 1 to mode 5; the maximum is then
701 considered to be the primary EOF mode; a value > 0 indicates the positive phase of the
702 EOF mode, and a value < 0 indicates the negative phase of the EOF mode.

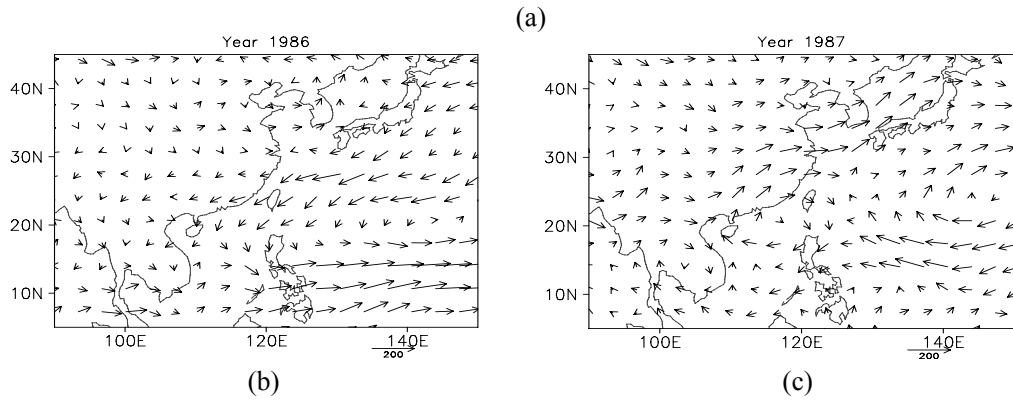
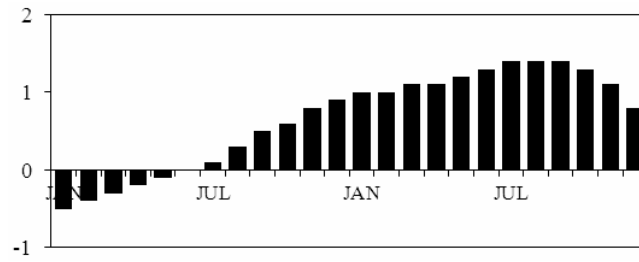
703



704

705 Fig. 7. (a) Time series of monthly SSTA anomalies over the Niño 3 region (unit: K) during
706 Jan 1983 to Dec 1984. Abnormal water vapor transport over East Asia-WNP in the
707 summer of (b) 1983, and (c) 1984.

708



709

710 Fig. 8. Same as Fig. 7, but for the period of Jan 1986–Dec 1987.

711

712 Table 1. Extreme years selected based on the PC1 and PC2 (greater/less than one standard
713 deviation), and their relationship with the SSTA over the tropical east-central Pacific.

	PC1	PC2
Positive(> δ)	1980* 1983* 1988** 1995** 1996 1998** 2007**	1980 1987** 1993** 2003**
Negative(< - δ)	1985 1986** 1990* 1997* 2002* 2004	1984** 1985** 1988 1989**

714

715 * PC1(+): the summer preceded by +SSTA and followed by -SSTA in the Niño 3 region; ** PC1(+):
716 the summer preceded by El Niño and followed by La Niña. Reverse for the case of PC1(-1); * PC2(+):
717 the summer in a developing +SSTA; ** PC2(+): the summer in a developing El Niño case. Reverse for
718 the case of PC2(-1).